water

MDPI

Supplementary materials:

S1. River Velocity, Dispersion, and Inflows

The i-Tree Cool River Model uses inputs of river discharge to solve for the advection and dispersion terms in Equation (1) as well as solve for the inflow reaction term, R_i in Equation (1) and (3). In unsteady conditions, such as during a storm, the model determines river velocity and dispersion using the one-dimensional St. Venant equation, which is solved numerically using the finite difference method given in Equations (3–25) to (3–29) by Boyd and Kasper [1]. This St. Venant finite difference method uses the Manning equation to relate velocity with river water depth, wetted perimeter, and cross-sectional area. The Manning equation operates in trapezoidal, triangular, or square channels with prescribed width, roughness, and side slope. The i-Tree Cool River Model uses a version of the Manning equation provided by Boyd and Kasper [1] in Equation (3–11). The Newton-Raphson root finding iterative method is used to solve the Manning equation and determine the adjusted wetted depth, hydraulic radius, wetted perimeter, cross-sectional area, and bottom width [1]. The i-Tree Cool River model uses the estimated velocity with the MacCormick method to determine the rate at which river water temperature travels between cross sections, using Equations (2–119) to (2–122) from Boyd and Kasper [1]. The St. Venant finite difference method requires compliance with Courant and frictional stability conditions for each node every timestep, using Equations (3–30) and (3–31) of Boyd and Kasper [1]. In steady state conditions, the model can determine velocity and dispersion using the St. Venant method, as done by Boyd and Kasper [1], or the user can select the Crank-Nicolson numerical method to solve a coupled set of velocity and temperature equations, following the approach of Zheng and Bennett, [2].

Inflows are composed of surface and subsurface sources. The surface inflow terms, Q_{ss} and T_{ss} of Equation (3) are input as a time series of flow rate (m^3/s) and temperature (°C), respectively, for any node receiving storm sewer, tributary, or other surface inflows. The flow and temperature values are either provided through measured observation or through estimation; we used observation in our study below.

The subsurface terms for groundwater inflow, Q_{GW} and T_{GW} of Equation (3) are input as a time series of groundwater flow rate (m^3/s) and temperature (°C) for each node and can be based on observation or estimation. The groundwater temperature was set to a constant 14.4 °C for the simulation period which was based on a function of annual average air temperature warming slightly in the summertime. Groundwater inflow was determined from observation, measuring baseflow at the upstream (station at the 0 m) and downstream (station at the 1500 m) sections of the Sawmill Creek during dry weather, and computing the inflow rate per unit length of the reach.

The subsurface hyporheic flow rate (m^3/s), Q_{Hyp}, and hyporheic flow temperature (°C), T_{Hyp} terms of Equation (3) for each node can be based on observation or estimation. Similar to groundwater flow, the hyporheic temperature was set to the constant 14.4 °C and hyporheic inflow was calculated in the i-Tree Cool River Model based on the Darcy Law [3] as

$$Q_{Hyp} = A_S K_S \frac{dh_D}{dx} \quad \text{(S1)}$$

where A_S is cross-sectional across seepage face (m^2), K_S is dominant substrate hydraulic conductivity (m/s), h_D is hydraulic head for Darcy calculation (m), and x is the model distance step (m).

S2. Heat Flux Calculations

S2.1a. Shortwave Radiation (First Method)

The model provides two methods for calculating shortwave radiation. The first method calculates the total shortwave radiation in Equation (4) is a function of the incoming solar radiation observed at the edge of the atmosphere [4], which i-Tree Cool River can calculate with two methods.

The first method is based on the albedo and a shading factor, which is based on the riparian vegetation condition along the river reach [5]

$$\Phi_{shortwave} = S_{in}(1-a)(1-SF) \tag{S2}$$

where S_{in} is incoming shortwave radiation, the sum of direct and diffuse shortwave radiation, a is the albedo (0 to 1), and SF is the estimated shading factor (0 to 1, with 1 for complete shade).

S2.1b. Shortwave Radiation (Second Method)

The second method for evaluating the shortwave radiation combines the adjusted direct and diffuse shortwave radiation, and uses sky view factors and shading width in place of a shading factor [6]

$$\Phi_{shortwave} = \Phi''^{direct}_{shortwave} + \Phi'^{diffuse}_{shortwave} \tag{S3}$$

The view-to-sky factor is applied to compute the topographic shading effect on diffuse solar radiation ($S^{diffuse}_{shortwave}$) [5]

$$\Phi'^{diffuse}_{shortwave} = S^{diffuse}_{shortwave}(1-a)\min(f_1, f_2, f_3) \tag{S4}$$

Direct shortwave radiation is computed using two steps, accounting for the width of shade across the river surface, and the river slope and aspect, as well as solar azimuth and altitude [6]

$$\Phi''^{direct}_{shortwave} = \Phi'^{direct}_{shortwave}\left(1-\frac{W'_{eff}}{W_{river}}\right) \tag{S5}$$

where W'_{eff} is the width of the effective shading and W_{river} is the river section wetted width, and are explained in the next paragraph, and $\Phi'^{direct}_{shortwave}$ is

$$\text{S2}\,\Phi'^{direct}_{shortwave} = S^{direct}_{shortwave}(1-a)[\sin\alpha\cos\varphi\cos(\beta-\theta_{\text{sun}})+\cos\alpha\sin\varphi] \tag{S6}$$

where $S^{direct}_{shortwave}$ is the incoming direct shortwave radiation, α is the longitudinal water surface slope (radians), β is the aspect with 0 set to true north (radians), θ_{sun} is solar azimuth angle (radians), indicating the angle of the position of the sun relative to true north, and φ is solar altitude (radians). The second method for calculating shortwave radiation, can reduce to the first method, in cases of full shade and full sun. For the case of full sun, the shade angle, SA = 0 and f_i = 1, resulting in $\Phi'^{diffuse}_{shortwave} = S^{diffuse}_{shortwave}(1-a)$ for Equation (S4), and the complementary term $\Phi''^{direct}_{shortwave}$, becomes $\Phi'^{direct}_{shortwave} = S^{direct}_{shortwave}(1-a)$ when $\varphi = \pi/2$ in equation (S6) and $W'_{eff} = 0$ in Equation (S5). For the case of full shade, the corollary occurs, with SA = 1 and f_i = 0, and $W'_{eff} = W_{river}$ in Equation (S6), resulting in no solar radiation on the river.

The total shadow width, W_{shade}, of near river objects, is calculated at each time step as a function of solar azimuth, altitude, and river azimuth (θ_{river}), in addition to object height at each node [6]

$$W_{shade} = (h_i)\left|\frac{\sin(\theta_{sun}-\theta_{river})}{\tan\varphi}\right| \tag{S7}$$

where the h_i is the combined height of the topography (i = 3) and building or vegetation bordering the river. When building and vegetation are present, the object is selected based on which has the largest shade angle SA from Equation (9) of the main text. The river width and distance from river to the shading object is compared with W_{shade} to determine the distances across the river surface covered in shade, and to determine the width of river effectively shaded, W_{eff} and the width of river directly under an overhanging object, $W_{overhang}$ such as tree canopy [5]. The model estimates the tree canopy width protruding from the tree trunk midpoint as 10% of the tree height [5]. The overhang is computed for either left or right banks [5]) as

$$W_{overhang} = \begin{cases} (0.1h_{tree} - D_{canopy})\rho_{veg} & \text{if } \left[(0.1h_{tree} - D_{canopy}) < W_{stream}\right] \\ W_{stream}\rho_{veg} & \text{if } \left[(0.1h_{tree} - D_{canopy}) \geq W_{stream}\right] \end{cases} \tag{S8}$$

where ρ_{veg} is the average density of the vegetation canopy, which ranges from 0 to 1 (unitless). The effective shading width is computed using Beer's Law as [5]

$$W_{eff} = \begin{cases} (W_{shade} - D_i - W_{overhang})(1 - e^{-\lambda L_{avg}}) & \text{if } SA_{veg} > SA_{i=1 or 3} \\ (W_{shade} - D_i - W_{overhang}) & \text{if } SA_{i=1 or 3} > SA_{veg} \end{cases} \tag{S9}$$

where λ, the radiation extinction coefficient, is calculated as a function of the leaf area index, *LAI* from the Equation (2) of DeWalle [7] and L_{avg} is the average path length of direct solar radiation through the shaded zone around the river (m) [6]. When canopy overhangs the river surface, the model uses an adjusted effective width W'_{eff} computed as

$$W'_{eff} = W_{eff} + W_{overhang} \tag{S10}$$

Using the adjusted direct radiation affected by topographic shading ($\Phi'^{direct}_{shortwave}$) and the calculated adjusted effective width, the net direct solar radiation affected by the topographic and shading barriers reaching to the surface, $\Phi''^{direct}_{shortwave}$ can be calculated as shown in Equation (S5) [6]

S2.2. Latent Heat Flux

The latent heat flux in Equation (4) of the main text is a negative upward flux representing evaporative cooling [8,9]. The latent heat flux is computed as [1]

$$\Phi_{latent} = -\rho L_e E \tag{S11}$$

where L_e is the latent heat of vaporization (J/kg), and *E* is the evaporation rate (m/s). The i-Tree Cool River Model provides two methods for calculation of *E* from open water, the Penman-Monteith combination method using Equation (30) of Westhoff et al. [9], and a mass transfer method using Equation (2–96) of Boyd and Kasper (2003).

S2.3. Sensible Heat Flux

Sensible convection of heat in Equation (4) of the main text represents the heat exchange between the surface of the water and the air [8]. The i-Tree Cool River Model provides three flexible methods to calculate the sensible heat flux, first and second methods (Equations (13) and (14)) based on the Bowen ratio of sensible to latent heat, and the third method (Equation (15) based on the sensible heat. The simpler of the two Bowen ratio methods is based on Boyd and Kasper [1]

$$\Phi_{sensible} = B_r \Phi_{latent} \tag{S12}$$

where *Br* is the Bowen ratio. The more complex of the Bowen ratio methods is based on Yearsley [10]

$$\Phi_{sensible} = B_r \rho_w \gamma N U_{wind} (T_{air} - T_w) \tag{S13}$$

where γ is the latent heat of vaporization (2.4995 × 10^6 J/kg), *N* is an empirical constant (1.59 × 10^{-9} s/m.mb) and U_{wind} is wind speed (m/s). The sensible-heat-based method considers wind speed as a driver of the convective flux, based on Dingman [11], given by Boyd and Kasper [1] as

$$\Phi_{sensible} = -K_H U_{wind} (T_w - T_{air}) \tag{S14}$$

where K_H is the heat exchange coefficient for sensible heat (J/m^3 °C).

S2.4. Bed Sediment Heat Flux

The bed sediment heat flux in Equation (4) of the main text is due to the heat conduction between the bed sediment and the water column and is rate limited by the size and conductance properties of the substrate. The approach modifies Equation (2-90) of Boyd and Kasper [1] as

$$\text{S2}\,\Phi_{se\,\text{dim}ent} = 2K_{CL}\frac{T_{bed} - T_w}{\frac{d_w}{2}} \tag{S15}$$

where K_{CL} is the volumetric weighted thermal conductivity (J/ms °C), T_{bed} is the bed temperature (°C), and d_w is the average river depth in the cross section (m). The sediment interface with the river water is the T_{bed} in Equation (S15); some applications prescribe T_{bed} to a depth below the interface. The sediment substrate in Sawmill Creek includes bedrock, boulders, cobbles, and gravels. Some boulders protrude above the water column, which is relatively shallow, and the unsubmerged sections of the sediment reach relatively high temperatures due to absorption of shortwave radiation. The mid-depth of the river, $d_w/2$, is used in Equation (S15) to represent a mid-point of the river water temperature reservoir. By solving for the heat fluxes of Equation (1) of the main text, the i-Tree Cool River Model can solve Equation (2) and provide the heat flux reaction term, R_e, for the governing advection-dispersion-reaction Equation (1) used to simulate river temperatures.

S3. Additional Sensitivity Analysis for Shading and Boundary Conditions

Shading along the riparian corridor modifies shortwave radiation, and patchiness in land cover then influences the land cover longwave radiation and longitudinal pattern in river warming when heat flux is the main driver of temperature. The NSRDB satellite estimated surface shortwave radiation was adjusted for each cross section based on the shading factor corresponding with that cross section (Figure S5). The shading factor along the 1500 m of Sawmill Creek reach was primarily a function of riparian tree shade from the canopy but was also a function of riparian topography and riparian building shade, which does include bridges crossing the river. When the shading factor was relatively small the shortwave radiation reaching the surface of Sawmill Creek was relatively large; for example values of radiation above 400 W/m^2 were associated with shade factors below 0.4. The shading factor used for each model node is observed at each cross sections, and between cross sections, there can be a considerable fluctuation between the minimum and maximum shading factors (see Figure S5). The upstream riparian corridors were more densely forested, while the downstream urbanized sections had intermittent coverage of buildings in the riparian corridors, and as a result, the shading factor tended to decrease from upstream to downstream. The river cross sections between the station 600 m and the station 900 m, where storm sewers contributed runoff from impervious areas, coincided with the large variation in the shade factor (Figure S5). Initially, the shading factors at cross section monitoring stations increased from 0.1 at 810 m to 1.0, the bridge, at 870 m, and then decreased to approximately 0.15 downstream of the urban section, at 1100 m. This increase in the shade factor from 0.1 to 1 about the bridge in the urban section of the reach reduced incoming shortwave radiation, which contributed to a mitigation of the thermal load delivered by urban runoff in this sub-reach.

The utilization of observed, i.e., recorded by a data logger, versus calculated upstream boundary conditions for water temperatures impacted simulation accuracy, which was a function of distance downstream and time of day (Figure S6). We examined the impact to our model simulation of changing the upstream boundary conditions from the recorded to the calculated upstream temperature. Impact was computed as delta temperature, $\Delta T_i = T_{observed} - T_{simulated}$, where the ΔT_i refers to $\Delta T_{recorded}$ when the boundary was recorded, and ΔT_{calc} when the boundary was calculated using the non-linear regression equation [12], and $T_{observed}$ is the observed temperature at each cross section, and $T_{simulated}$ is the simulated temperature at each cross section. We obtained $\Delta T_{recorded}$ and ΔT_{calc} for: (a) 01:00

h on 11 June 2007, selected as the mid-point between sunset to sunrise; and (b) 12:00 hours on 12 June 2007, selected as the mid-point between sunrise to sunset. In nighttime, $\Delta T_{recorded}$ varies about 0 °C throughout the reach, while ΔT_{calc} has a positive slope, trending from 1.0 °C upstream to 0.1 °C downstream in nighttime and trending from 0.9 °C upstream to 0.6 °C downstream. Comparison of the upstream cross section and downstream cross section differences indicated that running the model using the non-linear regression equation as the upstream boundary condition generated better simulations with distance downstream reache, moreso during nighttime than daytime.

Table S1. Observed water temperatures for three reaches of Sawmill Creek and for the Tannersville storm sewer, during 11 and 12 June 2007, as the average for all time steps during the dry or wet weather conditions.

Reach	Flow Type	Average Temperature (°C)
Upstream (0 m to 600 m)	Dry weather	15.1
	Wet weather	14.5
Middle (600 m to 900 m)	Dry weather	15.5
	Wet weather	14.8
Downstream (900 m to 1500 m)	Dry weather	15.6
	Wet weather	15.0
Storm sewer	Dry weather	14.9
	Wet weather	16.9

Table S2. List of the input files required for the simulation process of the i-Tree Cool River Model.

Input File	The Parameter Name	Description
BedData.dat	Number	The number of the observations indicates the locations of the observed streambed data.
	Distance (m)	Distances through the river reach where the streambed observations are recorded.
	Depth of Measurement (m)	Depth at which groundwater temperatures are recorded in each cross section
	GW_Temp (°C)	Groundwater temperature in downstream.
	Type	Bed-sediment type which can be clay, silt, sand, or gravel.
	Horizontal Bed Conductivity (mm/s)	Horizontal effective thermal conductivity in each observed cross-section.
	Bed Particle Size (mm)	Bed particle size in the observed location.
	Embeddedness (fraction)	Embeddedness in each considered cross section.
DEM.txt	Elevation data for calculating slope and aspect for calculating the hillslope effect on energy flux which can be converted from raster file to ASCII in Arc Map. The raw DEM data can be downloaded from the National Map Viewer.	
Discharge.dat	Number	The number of the observations indicates the locations of the observed groundwater data.

	Distance (m)	Distances through the river reach where the magnitude of groundwater flow is recorded
	Q_GW (cms)	Groundwater discharge.
Inflow.dat*	Number	The number of the observations which indicates the number of the time steps for the hydrographs of the river and lateral inflows.
	Inflow Rate Storm (cms)	Discharge rates of the river in upstream at each timestep defining the hydrograph in steady or unsteady mode.
	Inflow Temp Storm (°C)	Observed stream temperatures corresponding to the river hydrograph timesteps in upstream.
	Inflow Rate 1 (cms)	Discharge rates of the lateral storm sewer inflow at each timestep for the first location defining the hydrograph in steady or unsteady mode.
	Inflow Temp 1 (°C)	Observed stream temperatures corresponding to the first lateral storm sewer inflow hydrograph timesteps.
	Inflow Rate 2 (cms)	Discharge rates of the lateral storm sewer inflow at each timestep for the second location defining the hydrograph in steady or unsteady mode.
	Inflow Temp 2 (°C)**	Observed stream temperatures corresponding to the second lateral storm sewer inflow hydrograph timesteps.
	* The First row of the input file below the headings should be considered as the location of each hydrograph. The river's hydrograph gets 1 m indicating the upstream and other lateral inflows receive their own location from the upstream. ** The number of lateral inflows can be changed in the code by the user.	
Morphology.dat	Number	The number of the observations indicates the locations of the measured geomorphic data.
	Distance (m)	Distances through the river reach corresponding with the cross sections where the geomorphic data are recorded.
	Area (m^2)*	Cross-sectional wetted area of the river channel.
	Width (m)	Stream width.
	Depth (m)*	Wetted depth.
	Discharge (cms)	River discharge magnitude at the location where the geometric data are measured.
	Slope	Channel Slope

	Row#**	The row number in the DEM file where the cross-section is located.
	Column#**	The column number in the DEM file where the cross-section is located.
	Longitude (deg)**	Longitude of the cross-section in the geographic coordinate system.
	Latitude (deg)**	Latitude of the cross-section in the geographic coordinate system.
	Z (m)	The elevation of the cross-section.
	* Measured area and depth are required for running the Crank-Nicolson method in steady state. These parameters are calculated based on the depth using the Newton-Raphson root finding iterative method in explicit finite difference method. ** These input data are required for calculating the slope and aspect of each cell to apply the values on hillslope effect and the shortwave radiation. In case of using fixed magnitudes for the shading factor and view-to-sky values, these values are not effective in the simulation process.	
Shading.dat*	Number	The number of the observations reflecting the locations of the measured shading information.
	Distance (m)	Distances through the river reach corresponding with the cross sections where the shading information are recorded.
	EastBankH (m)	The height of the bankfull at the measured cross section on the Eastside.
	EastTreeH (m)	The height of the canopy at the measured cross section on the Eastside.
	EastBuildingH (m)	The height of the building at the measured cross section on the Eastside.
	EastBankDist (m)	Distance from the bankfull to the edge of the water at the measured cross section on the Eastside.
	EastCanDist (m)	Distance from the canopy to the edge of the water at the measured cross section on the Eastside.
	EastBuildingDist (m)	Distance from the building to edge of the water at the measured cross section on the Eastside.
	EastBufferW (m)	The magnitude of the canopy buffer at the location of the measured cross section on the Westside
	WestBankH (m)	The height of the bankfull at the measured cross section in the Westside.
	WestTreeH (m)	The height of the canopy at the measured cross section on the Westside.
	WestBuildingH (m)	The height of the building at the measured cross section on the Westside.
	WestBankDist (m)	Distance from the bankfull to the edge of the water at the measured cross section on the Westside.

	WestCanDist (m)	Distance from the canopy to the edge of the water at the measured cross section on the Westside.
	WestBuildingDist (m)	Distance from the building to edge of the water at the measured cross section on the Westside.
	WestBufferW (m)	The magnitude of the canopy buffer at the location of the measured cross section on the Westside
	Elevation (m)	The elevation of the cross-section.
	StreamAzimuth (deg)	The stream azimuth at the location of the measured cross section.
	* These input data are required for calculating the topographic, canopy (tree), and building shade angle and view-to-sky factor to apply the values to hillslope effect and the shortwave radiation. In case of using fixed magnitudes for the shading factor and view-to-sky values, these values are not effective in the simulation process.	
ShadingPercent.dat*	Number	The number of the observations reflecting the locations of the shading factors.
	Distance (m)	Distances through the river reach corresponding with the cross sections where the shading factor and the view-to-sky values are calculated.
	ShadeFactor	The value of shading factor in the desired cross-section.
	View-to-Sky	The value of View-to-Sky in the desired cross-section which is 1-shadingFactor
	* In case the topographic, canopy, and building heights and distances are considered for shading calculations, the magnitude of ShadingFactor and View-to-Sky are not effective in the simulation process.	
SolarRadiation.dat* The number of entries in this file should match the attribute value of totTime in the config file (see Table 2)	yyyymmdd	The date of the simulation period.
	Hr: Min: Sec	The time of the simulation period.
	DirSW (W/m^2)	Direct shortwave radiation at the edge of the atmosphere.
	DiffSW (W/m^2)	Diffuse shortwave radiation at the edge of the atmosphere.
	* Source: National Solar Radiation Database (NSRDB)	
Time.dat	Number	The number of the time steps.
	Time (s)	The desired time steps for the output intervals.
Weather.dat* The number of entries in this file should match the attribute value of totTime in the config file (see Table 2)	yyyymmdd	The date of the simulation period.
	Hr: Min: Sec	The time of the simulation period.
	Tair (F)	Air temperature.
	WndSpd (m/s)	Wind speed.
	Precip (m/h)	Precipitation rate.
	Cloudiness	The magnitude of the cloudiness.
	Humidity	Relative humidity.

	obsT_x0 (°C)	Observed river temperature in the upstream.
	sedT (°C)	Riverbed temperature.
	* National Center for Environmental Information	

Table S3. Statistical analysis (paired t-test) of the reach averaged observed and simulated river temperature in Sawmill Creek for the (a) original condition including both wet and dry weather (b) wet weather, and (c) dry weather.

Paired t-Test (a)
data: rawData$Orig_Obs and rawData$Orig_Mod t = 0.1593, df = 11, p-value = 0.8763 alternative hypothesis: true difference in means is not equal to 0 95 percent confidence interval: −0.02058636, 0.02379879 sample estimates: mean of the differences 0.001606213
Paired t-Test (b)
data: rawData$OrigStorm and rawData$ModStorm t = −0.43766, df = 11, **p-value = 0.6701** alternative hypothesis: true difference in means is not equal to 0 95 percent confidence interval: −0.06951900 0.04645744 sample estimates: mean of the differences −0.01153078
Paired t-Test (c)
data: rawData$OrigBaseQ and rawData$ModBaseQ t = 1.7253, df = 11, **p-value** = 0.1124 alternative hypothesis: true difference in means is not equal to 0 95 percent confidence interval: −0.01098885 0.09070502 sample estimates: mean of the differences 0.03985809

Table S4. Statistical analysis (paired t-test) of the reach averaged observed and simulated river temperatures using the scenarios for the (a) no shading effect, (b) no groundwater and hyporheic exchange inflows, and (c) calculated boundary condition.

Paired t-Test (a)
data: rawData$Observed and rawData$NoShading t = −9.8096, df = 11, **p-value = 8.955e-07** alternative hypothesis: true difference in means is not equal to 0 95 percent confidence interval: −0.4188181, −0.2653184 sample estimates: mean of the differences -0.3420683
Paired t-Test (b)
data: rawData$Observed and rawData$NoGWandHyp t = −6.6702, df = 11, **p-value = 3.514e-05** alternative hypothesis: true difference in means is not equal to 0 95 percent confidence interval: −0.19337108, −0.09741817 sample estimates: mean of the differences −0.1453946
Paired t-Test (c)
data: rawData$Observed and rawData$NoObsBC t = −11.553, df = 11, **p-value = 1.717e-07** alternative hypothesis: true difference in means is not equal to 0 95 percent confidence interval: −0.6902328, −0.4693167 sample estimates: mean of the differences −0.5797748

Table 5. Statistical analysis (paired t-test) of the observed and simulated river temperatures in Sawmill Creek, between 12:00 h of 11 Jun 2007 to 17:00 h of 12 June 2007.

Paired T-Test
data: rawData$ObsInTime and rawData$ModInTime t = 0.25605, df = 29, **p-value = 0.7997** alternative hypothesis: true difference in means is not equal to 0 95 percent confidence interval: −0.06101277, 0.07847554 sample estimates: mean of the differences 0.008731384

Table S6. Statistical analysis (paired t-test) of the observed and simulated river temperatures in Meadowbrook Creek, for 13–19 June 2012.

Paired T-Test
data: rawData$Observed and rawData$Simulated t = 0.35807, df = 116, **p-value = 0.7209** alternative hypothesis: true difference in means is not equal to 0 95 percent confidence interval: −0.05020794, 0.07236796 sample estimates: mean of the differences 0.01108001

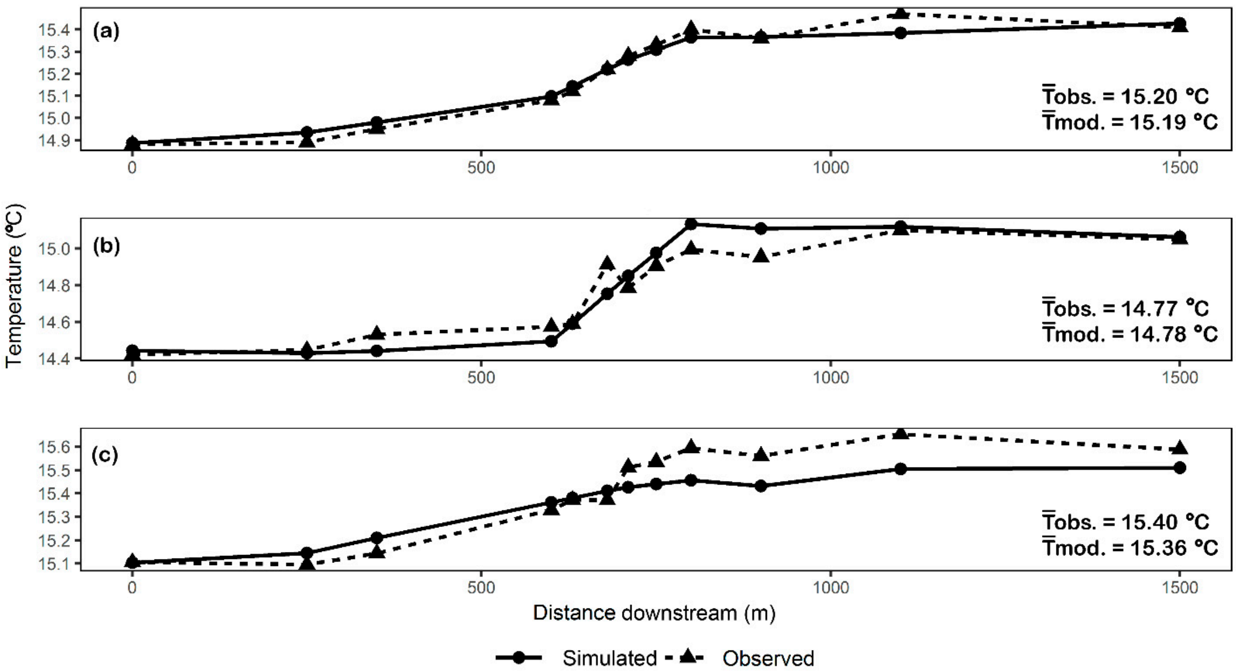

Figure S1. Time averaged observed and simulated river temperature in Sawmill Creek for the (**a**) original condition including both wet and dry weather (**b**) wet weather, and (**c**) dry weather.

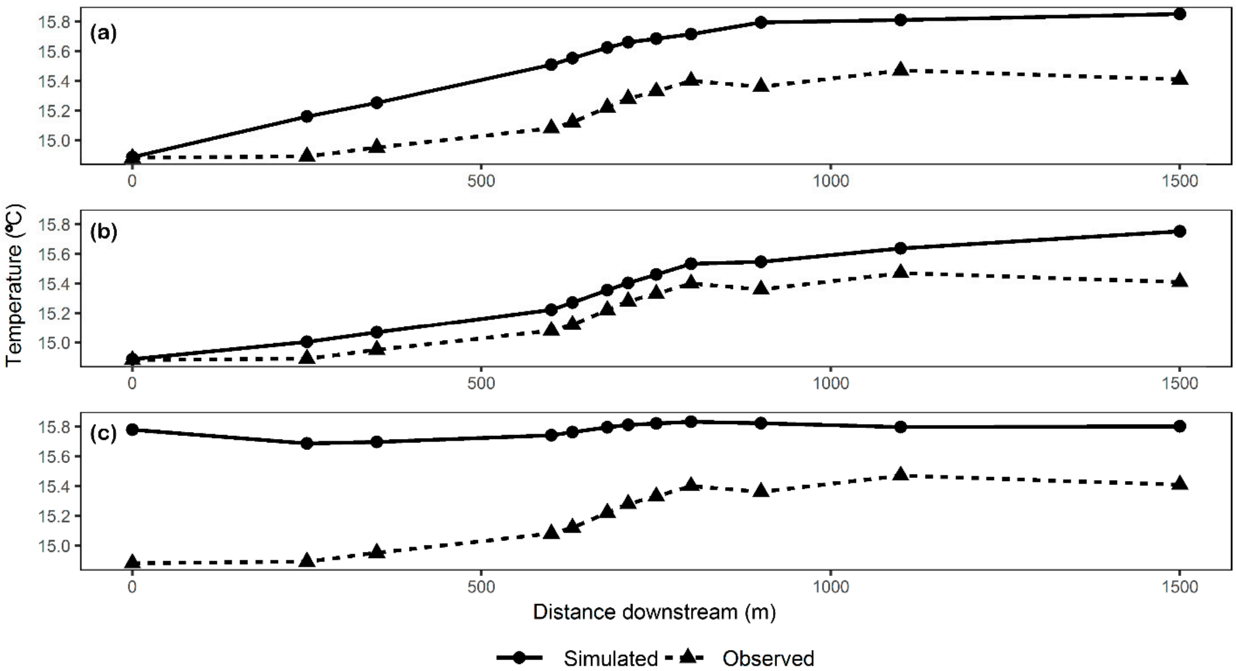

Figure S2. Time averaged observed and simulated river temperatures using the scenarios for the (**a**) no shading effect, (**b**) no groundwater and hyporheic exchange inflows, and (**c**) calculated boundary condition.

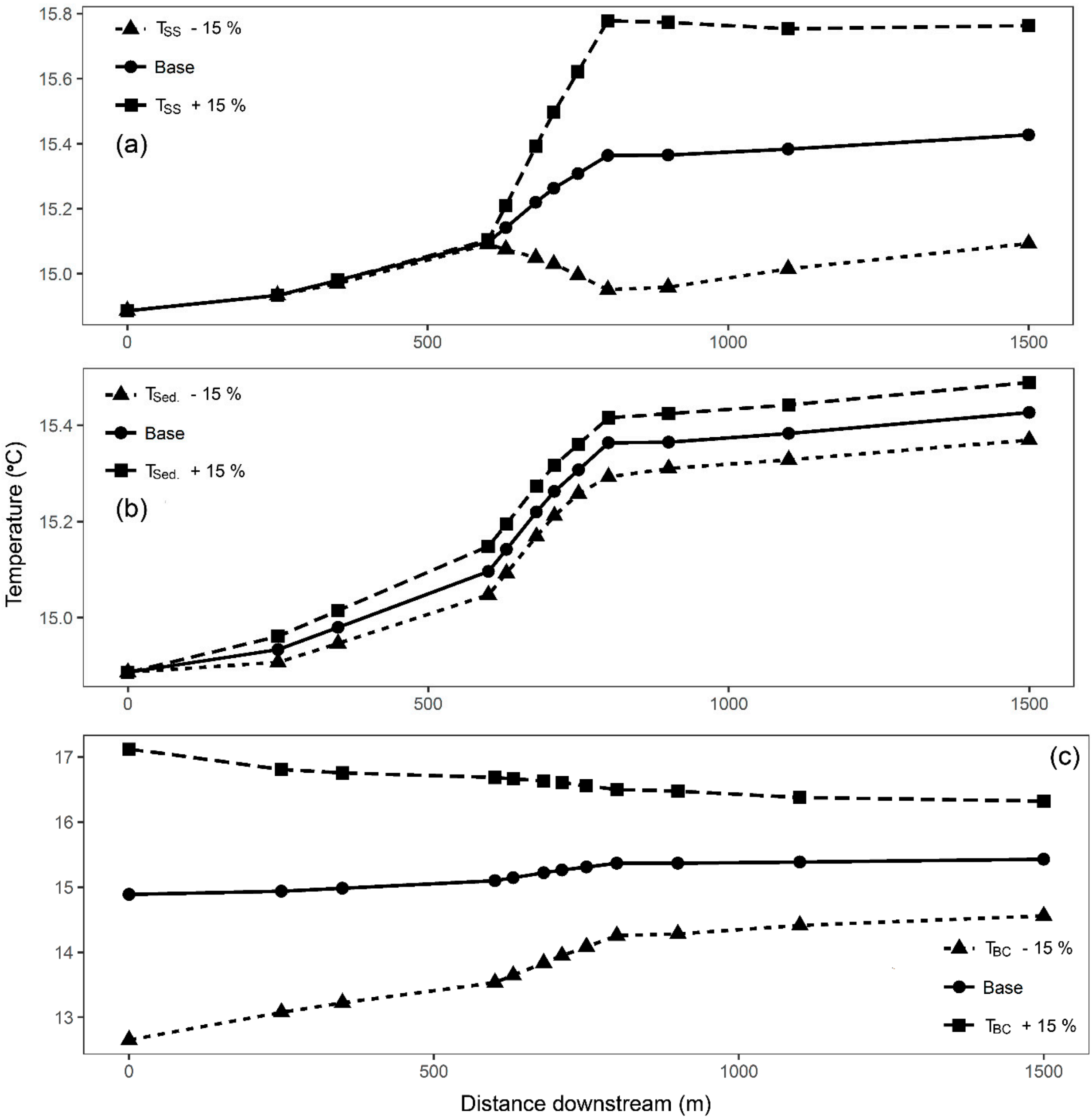

Figure S3. Simulated time averaged river temperatures along the 1500 m Sawmill Creek reach for the original condition (Base) and for conditions with ±15% changes in (**a**) storm sewer temperature (T_{SS}), (**b**) sediment temperature, and (**c**) boundary conditions temperature.

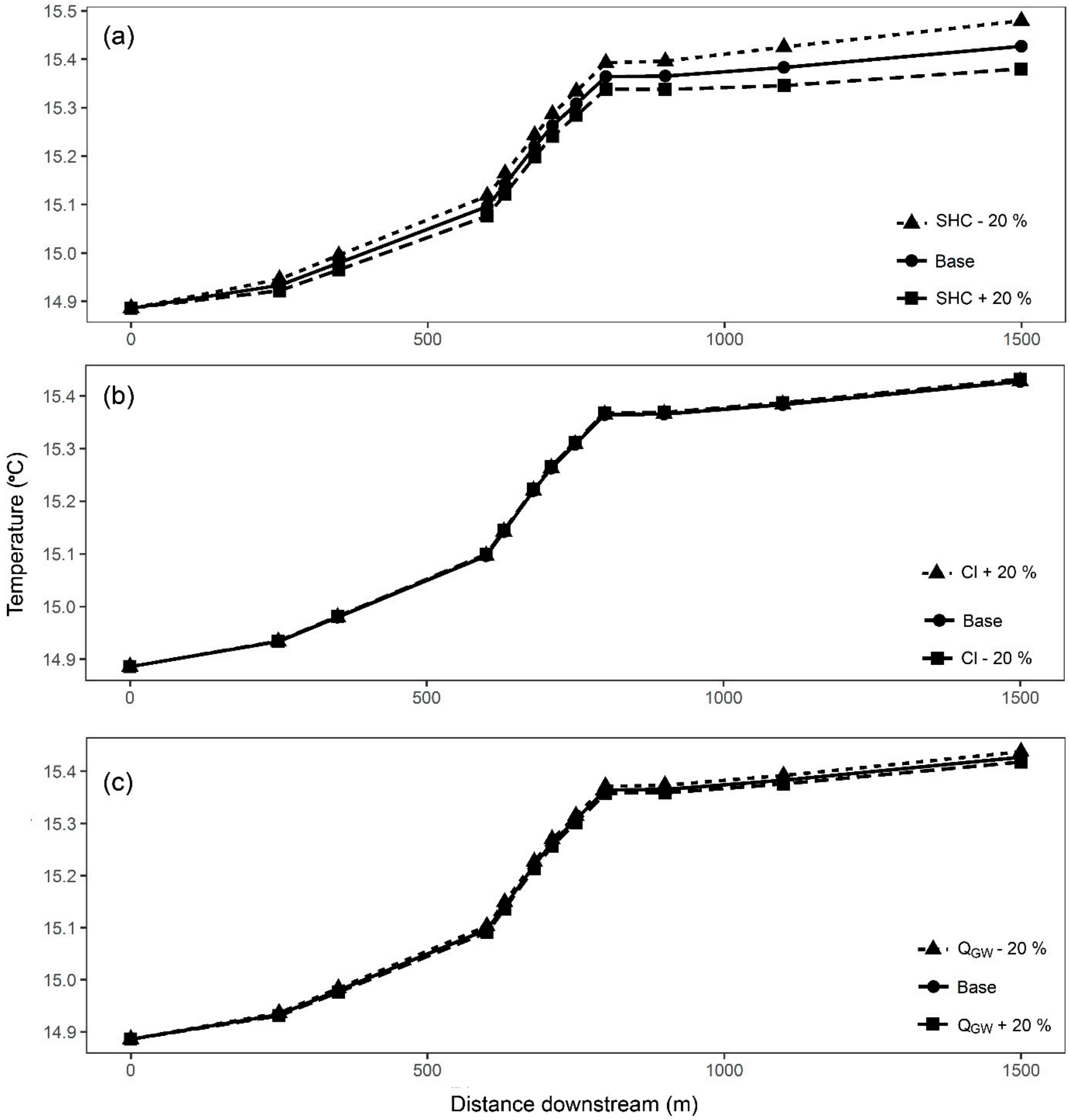

Figure S4. Simulated time averaged river temperature along the 1500 m Sawmill Creek reach for the original condition (Base) and for conditions with ±20% changes in (**a**) substrate hydraulic conductivity (SHC), (b) cloudiness factor (Cl), and (c) groundwater discharge (GW).

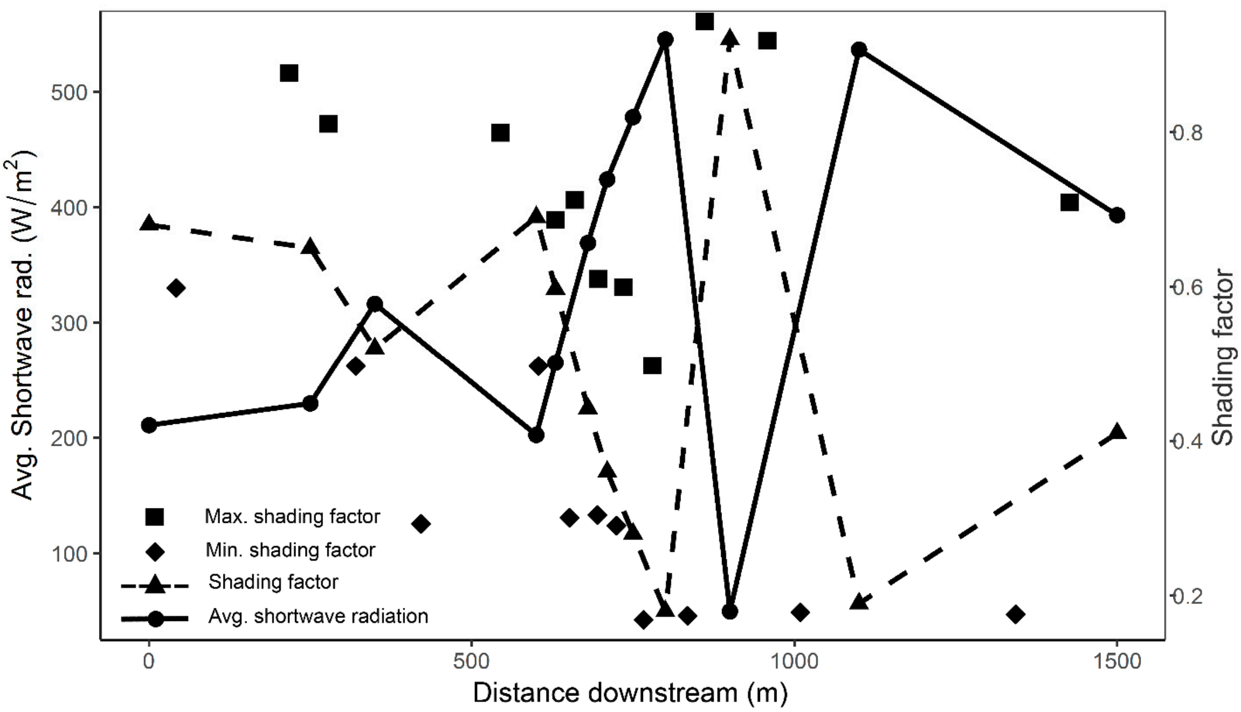

Figure S5. Fluctuations of shading factors and daily average shortwave radiation along the 1500 m Sawmill Creek reach. The shading factors denoted by a triangle are measured at each of the 12 monitoring stations, and the minimum and maximum shading factors were selected from the 5 m interval set of shading factors measured between each station.

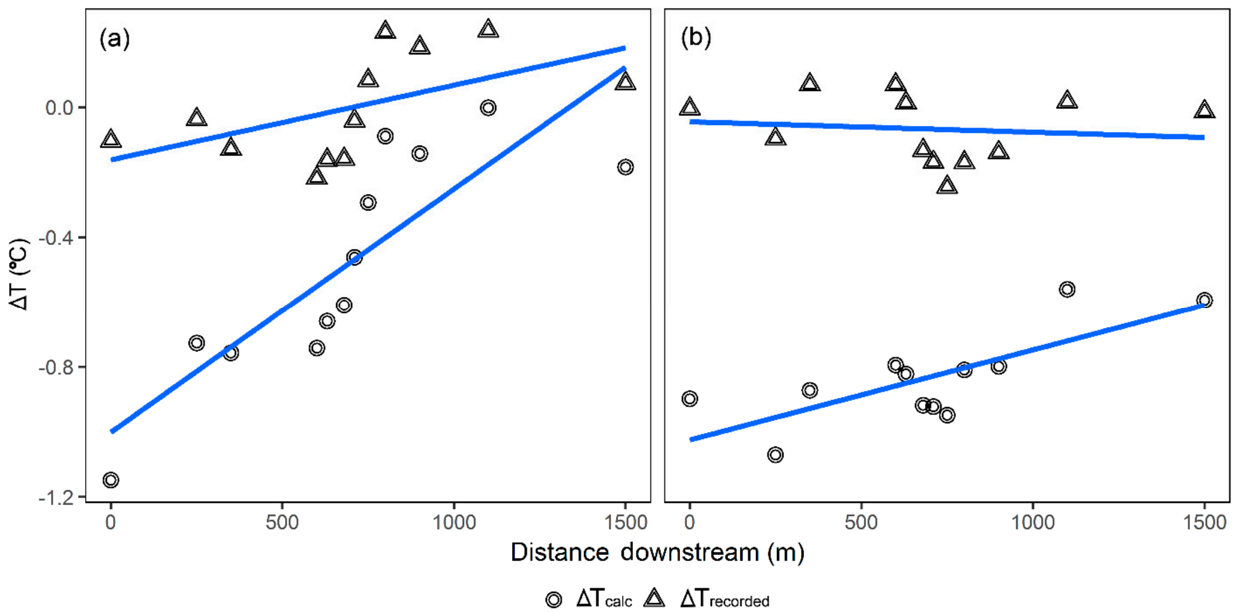

Figure S6. Temperature differences between the observed and simulated river temperature when using Mohsni et al. (1998), ΔT_{calc} versus recorded, $\Delta T_{recorded}$ boundary conditions, for (**a**) nighttime and (**b**) daytime.

References:

1. Boyd, M.; Kasper, B. *Analytical Methods for Dynamic Open Channel Heat and Mass Transfer: Methodology for Heat Source Model Version 7.0*; Watershed Sciences Inc: Portland, OR, USA, 2003.
2. Zheng, C.; Bennett, G.D. *Applied Contaminant Transport Modeling*; Van Nostrand Reinhold: New York, NY, USA, 1995.

3. Domenico, P.A.; Scwartz, F.W. *Physical and Chemical Hydrogeology*; John Wiley and Sons, Inc.: New York, NY, USA, 1990.
4. Ouellet, V.; Secretan, Y.; St-hilaire, A.; Morin, J. Water temperature modelling in a controlled environment: Comparative study of heat budget equations. *Hydrol. Process*. **2014**, *28*, 279–292.
5. Chen, Y.D.; Carsel, R.F.; McCutcheon, S.C.; Nutter, W.L. Stream temperature simulation of forested riparian areas: I. Watershed-Scale model development. *J. Environ. Eng*. **1998**, *124*, 304–315.
6. Sun, N.; Yearsley, J.; Voisin, N.; Lettenmaier, D.P. A spatially distributed model for the assessment of land use impacts on stream temperature in small urban watersheds. *Hydrol. Process*. **2015**, *29*, 2331–2345.
7. DeWalle, D.R. Modeling stream shade: Riparian buffer height and density as important as buffer width. *J. Am. Water Resour. Assoc*. **2010**, *46*, 323–333.
8. Webb, B.; Zhang, Y. Spatial and seasonal variability in the components of the river heat budget. *Hydrol. Process*. **1997**, *11*, 79–101.
9. Westhoff, M.C.; Savenije, H.H.G.; Luxemburg, W.M.J.; Stelling, G.S.; Giesen, N.C. Van De, Selker, J.S. Sciences A distributed stream temperature model using high-resolution temperature observations. *Hydrol. Earth Syst. Sci*. **2007**, *11*, 1469–1480.
10. Yearsley, J.R. A semi-Lagrangian water temperature model for advection-dominated river systems. *Water Resour. Res*. **2009**, *45*, W12405.
11. Dingman, S.L. *Physical Hydrology*; Prentice-Hall Inc.: Upper Saddle River, NJ, USA, 1994.
12. Mohseni, O.; Stefan, H.G.; Erickson, T.R. A nonlinear regression model for weekly stream temperatures. *Water Resour. Res*. **1998**, *34*, 2685–2692.